

ERASMUS UNIVERSITY ROTTERDAM

ERASMUS SCHOOL OF ECONOMICS

MASTER'S THESIS QUANTITATIVE FINANCE

Scenario Based Policy Research Under Parameter Uncertainty

AUTHOR

Michael Darmoutomo (432977)

SUPERVISOR

dr. Reuvers, J.W.N.

SECOND ASSESSOR

dr. Kole, H.J.W.G.

April 29, 2022

Abstract

This paper takes a look at the effect of parameter uncertainty on scenario based policy research. More specifically, we extend an earlier research where welfare gains are claimed to be obtained when risk is allocated age-dependently in the Dutch pension system. We compare three age-dependent risk allocations and compare it with a uniform adjustment. The allocations are evaluated under two different economic scenario sets, one including, and one excluding parameter uncertainty. We no longer find significant welfare gains when we incorporate parameter uncertainty in the scenario sets.

Contents

1	Introduction	3
2	Literature	5
3	Data	7
4	Methodology	9
4.1	KNW-model	9
4.1.1	Nominal Interest Rates	10
4.2	State-Space Formulation of KNW-model	10
4.2.1	Discretisation	12
4.2.2	Likelihood Function	13
4.2.3	Prior Initialisation	13
4.2.4	Restrictions	14
4.3	Parameter Uncertainty	14
4.4	Pension Fund	15
4.5	Risk Allocation	17
4.5.1	3-2-1 Adjustment Rule	18
4.5.2	Uniform Adjustment to Achievable Pension	18
4.5.3	Optimisation over the Life Cycle	19
4.6	Measuring Welfare	19
4.6.1	Standard Error	21
4.7	CEC Analysis	21
5	Results	21
5.1	Parameter Estimates	23
5.2	Economic Scenarios	23
5.3	Pension Fund Simulation	24
5.3.1	Adjustment Factors	25
5.3.2	Robustness Checks	26
5.3.3	Effect of Factors	28
6	Discussion	29
7	Conclusion	31

Appendices	36
A Code structure	37
B Scenario sets	39

1 Introduction

Financial markets are complex and heavily interconnected with the real economy. To better understand this complex world, mathematical tools have been developed to describe financial and economical processes. These models can describe the behaviour of stock prices, inflation, bond prices, etc. given market data. However, they are not limited to only describe economic processes, but can be extended to generate new data. Generating different economic scenarios can be useful to price complicated derivatives, research effects of (monetary) policy changes, or for risk management of financial institutions. These scenarios give possible future paths for financial markets or economies.

One particular model to describe the economy is the Koijen-Nijman-Werker (KNW) model (Koijen et al., 2010). Committee Parameters (Langejan et al., 2014) and Dijsselbloem et al. (2019) advice to use this model to generate economic scenarios for pension funds. This capital market model describes the dynamics of a stock index, interest rates and inflation. Pension funds are under strict regulations of central banks. The Dutch Central Bank (DNB) publishes a scenario set of 10,000 scenarios every quarter that pension funds have to use for their feasibility tests. The calibration of the KNW-model is performed with new incoming data every quarter. Draper (2012) and Muns (2015) introduce an adjusted version of the Kalman Filter to calibrate the KNW-model. On the other hand, Pelsser (2019) proposes to rewrite the state-space formulation such that a conventional Kalman filter can be used to estimate the KNW-model.

The economic scenarios extend their functionality beyond feasibility tests. Changes in pension policies need to be considered very carefully as it affects a large share of the population. Participation in a pension fund in the Netherlands is often mandatory. The Dutch pension system is one of the best in the world¹. The system consists of three pillars. The first pillar is the General Old-Age Pensions Act (AOW), which is a Dutch basic state pension everyone receives. The second pillar is the company pension that is accumulated during one's working life, and usually consists of a share of your wage and a contribution by your employer. Finally, the third pillar consists of personal savings and insurance products. In the second pillar, employees and employers pay the contribution into a collective pension fund to which the employer is affiliated. At the age of 67 the retiree can claim a monthly benefit of the fund.

The research on life cycle investing is extensive. Pension funds play a crucial role in people's end-of-period wealth. Bovenberg et al. (2007) provide an extensive survey on life cycle investing and the role of collective pension funds. Collective investment schemes allow for more flexible risk sharing. Whereas individual investments can only share risks traded on the financial mar-

¹<https://www.mercer.com.au/our-thinking/global-pension-index.html>

ket, collective schemes can share the risk across different generations (Boelaars et al., 2015). Bovenberg et al. (2007) show that one can obtain welfare gains by allowing for age dependent risk allocation. An important question remains, what is the optimal method to spread out the investment risks? One method is proposed by Lever and Michelsen (2016), where they share risk by spreading out shocks across multiple years. This leads to so-called implicit age differentiation. Another method is explicit age differentiation. Chen et al. (2019) provide an extensive comparison between different age-dependent risk allocations. They consider three different allocation functions, which all offload most risk on younger generations. Two of the methods are age dependent and one directly proportional to the built up pension.

Chen et al. (2019) and Darmoutomo et al. (2020) use the KNW-model to generate different economic scenarios and evaluate the welfare gains of different cohorts. They use the estimated parameters by the Dutch Central Bank to simulate different paths for the economy and financial market. However, model parameters come along with parameter uncertainty. Due to the fact that we cannot observe the real data generating process, but simply samples of this noisy data, we know that we cannot be certain that the estimates describe the true economy. In this research we propose to extend Chen et al. (2019) and perform an additional robustness check on the obtained welfare gains and losses. We will estimate the KNW-model using the framework of Pelsser (2019) and generate new scenarios while incorporating parameter uncertainty.

The methodology of this thesis will be two-fold. First, we will estimate the KNW-model and the estimation errors using a Kalman Filter, secondly we will model a pension fund and see how the welfare gains or losses are affected for different risk allocation strategies by incorporating parameter uncertainty.

We show that, in line with earlier research, age dependent risk sharing leads to substantial welfare gains. In accordance with Chen et al. (2019), we find that the 3-2-1 distribution rule leads to a welfare loss of around 1.79% compared to age independent risk sharing. But the more flexible methods such as the uniform adjustment in achieve pension and optimisation over the life cycle lead to significant welfare gains of around 2.59% and 3.08% respectively. However, when we extend their research and consider parameter uncertainty for the estimated KNW-model parameters, we find different results. The uniform adjustment in achievable pension only leads to a welfare gain of around 0.93% and the optimisation over the life cycle leads to a welfare loss of around 0.46%. Both methods are no longer significantly different from zero. Also the 3-2-1 distribution rule leads to a welfare loss of around 2.10%. We thus find that the welfare gains obtained by Chen et al. (2019) are rather arbitrary, and that parameter uncertainty in the model affects their inference. Including parameter uncertainty in the economic

scenario generator results in fatter tails. Hence more extreme returns are more likely to happen. Offloading extra risk on the younger generations could potentially cause a decrease in certainty equivalent of consumption. Especially when we do not consider the likelihood of big negative shocks and negative interest rates. Certain cohorts will not sufficiently recover from bad periods at their retirement age. Thus, policy makers should consider the uncertainty in parameters for changing their system.

The remainder of this thesis is structured as follows. Section 2 introduces the reader to some background information about life cycle investing and the role of pension schemes. Section 3 describes the data that is used to calibrate the KNW-model. Section 4 gives a thorough description of the methods used. It describes the details about the KNW-model and the estimation procedure, how the asset liability management simulations are performed and how welfare is measured for different risk allocation methods. Section 5 shows the estimation results and obtained welfare gains and losses. Finally, we discuss our results and possible limitations in Section 6 and conclude this thesis in Section 7.

2 Literature

The optimal allocation of an individual's portfolio over time is often motivated by the life cycle model introduced by Modigliani (1966). An individual's capital is build up of human capital as well as financial capital. Human capital is the discounted earned income during their working life. For young individuals this value is high. Over time the human capital will decrease as there is less time left to work. The financial capital slowly increases over one's life-time until retirement age and then decreases when their capital is used to keep up the consumption level during this period.

In life cycle theory it is assumed that human capital grows at a constant rate and is risk-free. Therefore, an individual can invest part of his financial capital into financial markets to receive a risk premium. The underlying assumption is that we are willing to expose ourselves to some extra risk in exchange for higher returns. Merton (1969, 1975) and Samuelson (1975) show that it is optimal to expose a constant fraction of our wealth to risky assets. When the individual gets older a larger part of their wealth will consist of financial capital and less of the risk-free human capital. Therefore to maintain the same risk exposure, it will be beneficial to decrease the exposure to risky assets.

One critical assumption of these models is that human capital is risk-free and uncorrelated with equity returns, however in practice this does not always hold. First, an individual can get promoted, get sick, lose their job, or start their own business. Second, Viceira (2001) and

Benzoni et al. (2007) show that in fact human capital and equity risk are correlated. This is because both human capital and equity risk affect the gross domestic product. The correlation between human capital and the stock market lowers the optimal fraction that should be exposed to risky assets (Boelaars and Mehlkopf, 2018).

Young people have a larger fraction of their total capital in human capital, they have a longer horizon to compensate for economic shocks. They can simply work more or less (Bodie et al., 1992), adapt their future pension benefits or increase their retirement age (Gomes et al., 2008). Therefore, the hypothesis is that welfare gains can be achieved by exposing young people to more risk than older people.

In the Netherlands, pension funds play a crucial role in building up a person's wealth. They provide participants the opportunity to collectively invest into a fund. The pension scheme has several benefits, such as providing financial expertise which participants might lack to perform financial planning and reducing the cost for life cycle planning (Bovenberg and Meijdam, 2001). Next to this, pension funds enable risk sharing across non-overlapping generations which smooths out consumption. Bovenberg et al. (2007) provide an extensive survey on life cycle investing and the role of collective pension funds. However, pension funds deal with a large number of participants with different characteristics. According to the life cycle theory, younger generations should be exposed to more risk due to their large human capital, and older generations to less. Therefore, it is suboptimal for pension funds to have a uniform investment strategy for their participants. Teulings and De Vries (2006) introduced the idea of generational accounts. All contributions by one generation are paid into the same account. The benefits would be paid out using this account to the generation that contributed to the account when they retire. Consequently, we can have an investment strategy that fits the life cycle of each generation.

In practice, some age-differentiation is already present in the Dutch pension scheme. Shocks in the financial market are spread out over several years to reduce the effect on changes in benefits. This results in so-called implicit age-differentiation (Boelaars et al., 2015; Mehlkopf et al., 2013). Spreading out the shocks also shares the risk with future generations, which smooths out consumption as well. Lever and Michelsen (2016) shows implicit age-differentiation can lead to substantial welfare gains. Another methodology is called explicit age-differentiation, where we no longer make changes to indexation uniformly, but dependent on age. For example, a pension fund with a lot of old generations will probably take too little risk for the younger generations and vice versa. Bovenberg et al. (2007) shows that an age-dependent allocation rule results in substantial welfare gains, compared to a uniform rule. Chen et al. (2019) provide an extensive comparison between different age-dependent risk allocations. Their first rule is a

3-2-1 rule, where shocks to young generations are three times as large as to older people, and two times as large to middle-aged generations. The second allocation rule is that shocks are allocated uniformly to the achievable pension as introduced by Muns and Werker (2019). The last method consists of an optimisation method, where the shocks are allocated depending on a mathematical allocation rule. They find considerable welfare gains for the last two methods.

3 Data



Figure 1: MSCI and HICP data. This figure shows the HICP and MSCI index. The grey areas denote recessions periods in the Netherlands. The recession periods are based on OECD data. Data can be retrieved from <https://fred.stlouisfed.org/series/NDLREC>.

The KNW-model describes inflation, interest rates and equity returns. A description of the data used by the Dutch Central Bank can be found in the Appendix of Committee Parameters (2019). We will extend the used data to September 2021. However, some data is unavailable to us, therefore we only use data from January 2004 until September 2021. This paper will consider monthly stock price, bond price and inflation data.

- For inflation, we use the Harmonized Index of Consumer Prices (HICP) for the euro area from the European Central Bank (ECB). The data is obtained from the website of the ECB (ICP.M.U2.Y.000000.3.INX)². The data ranges from January 1999 to September 2021 and consists of 273 observation.
- For the yields, we consider zero coupon rates published by the Dutch Central Bank. The

²<https://sdw.ecb.europa.eu/browse.do?node=9691215>

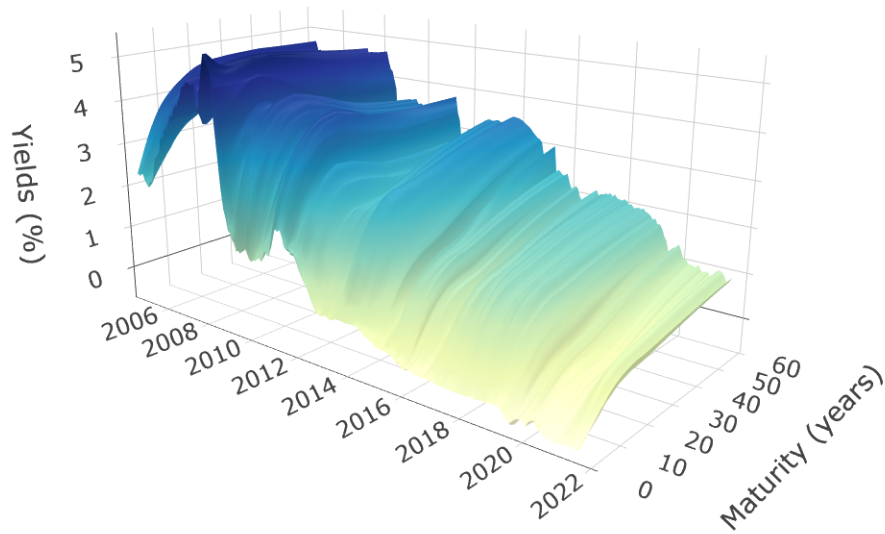


Figure 2: Yield surface. This figure shows yields with maturities ranging from 1 to 60 years over the period January 2004 – September 2021.

data is obtained from <https://www.dnb.nl/statistieken> and ranges from December 2001 to September 2021. We got maturities ranging from 1-60 years for the period of December 2001 to December 2014, and maturities ranging from 1-100 years for the period of January 2015 to September 2021. Monthly data is only available from January 2004.

- For the stock market, we consider the Morgan Stanley Capital International (MSCI) index ranging from January 1999 to September 2021. We consider monthly returns. The monthly returns can be retrieved from Bloomberg.

Figure 1 shows the HICP and MSCI index from January 2004 until September 2021. The OECD data shows four recession periods during this time period. The HICP index has an average annual growth of around 1.5 percent. Figure 2 shows the evolution of yields during the period of January 2004 to September 2021 with maturities ranging from 0 to 60 years. We observe a declining trend in yields over the years since the financial crisis and the short-term yields are getting close to zero. The yield characteristics are clearly visible in the last few years. The curve shows higher yields for higher maturities and lower yields for the shorter maturities.

The data is transformed for estimation purposes. Rather than taking the actual values of the HICP and MSCI index, we use their log values. We also shift the HICP and MSCI index such that their first observation is set to zero. We will only take the 1, 5, 10, 15, 20 and 30 years maturities into consideration.

4 Methodology

This section will introduce all necessary theory and methodology to estimate the KNW-model and analyse the effect of different risk allocations within a pension fund. The section is two-fold. First, Sections 4.1 – 4.3 describe the KNW-model and our estimation process. Second, Sections 4.4 – 4.6 describe how we model the pension fund and measure welfare gains or losses for different risk allocation methods.

4.1 KNW-model

The Kojien-Nijman-Werker (KNW) model (Kojien et al., 2010) is a two-factor Gaussian affine model for interest rates and inflation, combined with a generalised Black-Scholes (GBM) model for stock prices. The dynamics of equity returns, interest rates and inflation are governed by two state variables X_{1t} and X_{2t} . The process $X_t = [X_{1t}, X_{2t}]'$ follows a mean reverting process around zero and the dynamics of the states are described by the following stochastic differential equation (SDE)

$$dX_t = -KX_t dt + d\tilde{W}_t^{\mathbb{P}}, \quad (1)$$

where K is a normalised lower triangular 2×2 matrix to keep the model identifiable (Dai and Singleton, 2000) and $\tilde{W}_t^{\mathbb{P}}$ is a two-dimensional \mathbb{P} -Brownian motion, with \mathbb{P} denoting the real-world probability measure. The model describes the instantaneous nominal interest rate (r_t) and the instantaneous expected inflation (π_t) as an affine function in state variable X_t :

$$r_t = \delta_{0R} + \delta'_{1R} X_t, \quad (2)$$

$$\pi_t = \delta_{0\pi} + \delta'_{1\pi} X_t. \quad (3)$$

The price index (Π_t) and stock index (S_t) evolve as

$$\frac{d\Pi_t}{\Pi_t} = \pi_t dt + \sigma'_{\Pi} dW_t^{\mathbb{P}}, \quad \sigma_{\Pi} \in \mathbb{R}^4 \text{ and } \Pi_0 = 1, \quad (4)$$

$$\frac{dS_t}{S_t} = (r_t + \eta_S) dt + \sigma'_S dW_t^{\mathbb{P}}, \quad \sigma_S \in \mathbb{R}^4 \text{ and } S_0 = 1, \quad (5)$$

with η_S the equity risk premium and $dW_t^{\mathbb{P}}$ a 4-dimensional \mathbb{P} -Brownian motion. To keep the model well-identified, we impose $\sigma_{\Pi,(4)} = 0$ as suggested by Chen et al. (2019). Finally, the nominal stochastic discount factor, ϕ_t^N , is described as

$$\frac{d\phi_t^N}{\phi_t^N} = -r_t dt - \Lambda'_t dW_t^{\mathbb{P}},$$

with the price of risk at time t , and Λ_t equal to

$$\Lambda_t = \Lambda_0 + \Lambda_1 X_t \text{ with } \Lambda_t, \Lambda_0 \in \mathbb{R}^4 \text{ and } \Lambda_1 \in \mathbb{R}^{4 \times 2}. \quad (6)$$

As we assume that the risk premium is constant, we have $\sigma'_S \Lambda_t = \eta_S$. This puts restrictions on the parameters Λ_0 and Λ_1 . The assumption implies that $\sigma'_S \Lambda_1 = 0$ and $\sigma'_S \Lambda_0 = \eta_S$. Another assumption is that there is no risk premium for unexpected inflation risk, thus $\Lambda_{0,(3)} = 0$ and $\Lambda_{1,(3)} = 0$, where $\Lambda_{1,(3)}$ denotes the third row.

4.1.1 Nominal Interest Rates

Following the derivation of Kojien et al. (2010), the price of a zero-coupon rate bond at time t with maturity τ is equal to

$$P_t(\tau) = \exp(-A(\tau) - B(\tau)'X_t), \quad (7)$$

with

$$B(\tau) = (K + \Lambda_1)'^{-1}(I_k - e^{-(K+\Lambda_1)'\tau})\delta_{1r}, \quad (8)$$

$$A(\tau) = \int_0^\tau \delta_{0r} - \lambda'_0 B(s) - \frac{1}{2}B(s)'B(s)ds. \quad (9)$$

The corresponding yield, $y_t(\tau)$, is equal to $\frac{A(\tau)}{\tau} + \frac{B(\tau)'}{\tau}X_t$.

4.2 State-Space Formulation of KNW-model

In contrast to Draper (2014) and Muns (2015), who use a non-standard Kalman filter, Pelsser (2019) proposes to rewrite the KNW-model so that a standard Kalman filter can be used. We can achieve this by augmenting the state variables X_t . We include the log of the price index and stock market into our augmented state variable $\tilde{X}_t = (X_t, \ln \Pi_t, \ln S_t)$. The dynamics of \tilde{X}_t are then given by

$$d\tilde{X}_t = \left[\underbrace{\begin{pmatrix} 0_{1 \times k} \\ \delta_{0\pi} - \frac{1}{2}\sigma'_{\Pi}\sigma_{\pi} \\ \delta_{0R} + \eta_S - \frac{1}{2}\sigma'_S\sigma_S \end{pmatrix}}_{\Theta_0} + \underbrace{\begin{pmatrix} -K & 0_{k \times 2} \\ \delta'_{1\pi} & 0_{1 \times 2} \\ \delta'_{1R} & 0_{1 \times 2} \end{pmatrix}}_{\Theta_1} \begin{pmatrix} X_t \\ \ln \Pi_t \\ \ln S_t \end{pmatrix} \right] dt + \underbrace{\begin{pmatrix} [I_k & 0_{k \times 2}] \\ \sigma'_{\Pi} \\ \sigma'_S \end{pmatrix}}_{\Theta_2} dW_t^{\mathbb{P}}. \quad (10)$$

The above stochastic differential equation (SDE) is known as an Ornstein–Uhlenbeck process of the form $d\tilde{X}_t = (\Theta_0 + \Theta_1\tilde{X}_t)dt + \Theta_2dW_t^{\mathbb{P}}$. For a small time step Δt , Pelsser (2019) derives the

following transition density

$$\tilde{X}_t | \tilde{X}_{t-\Delta t} \sim \mathcal{N} \left(\int_0^{\Delta t} e^{\Theta_1 u} \Theta_0 du + e^{\Theta_1 \Delta t} \tilde{X}_{t-\Delta t}, \int_0^{\Delta t} e^{\Theta_1 u} \Theta_2 \Theta_2' e^{\Theta_1' u} du \right). \quad (11)$$

It follows directly from (11) that the VAR(1)-representation of \tilde{X}_t becomes

$$\tilde{X}_t = \phi + \Phi \tilde{X}_{t-\Delta t} + \varepsilon_t, \quad \text{Var}(\varepsilon_t) = R, \quad (12)$$

with vector $\phi = \int_0^{\Delta t} e^{\Theta_1 u} \Theta_0 du$, matrices $\Phi = e^{\Theta_1 \Delta t}$ and $R = \int_0^{\Delta t} e^{\Theta_1 u} \Theta_2 \Theta_2' e^{\Theta_1' u} du$. This equation will be referred to as the state equation.

Let $y_t \in \mathbb{R}^m$ be a vector of zero-coupon rates with maturities of τ_1, \dots, τ_m . Then, we also augment the observation variable $\tilde{y}_t = (y_t, \ln \Pi_t, \ln S_t)$. The measurement equation is then defined as

$$\tilde{y}_t = \begin{pmatrix} y_t \\ \ln \Pi_t \\ \ln S_t \end{pmatrix} = a + B \tilde{X}_t + w_t, \quad \text{Var}(w_t) = Q, \quad (13)$$

with $a \in \mathbb{R}^{(m+2)}$ and $B \in \mathbb{R}^{(m+2) \times (k+2)}$ defined as

$$a = \begin{pmatrix} A(\tau_1)/\tau_1 \\ \vdots \\ A(\tau_m)/\tau_m \\ 0 \\ 0 \end{pmatrix}, \quad B = \begin{pmatrix} B(\tau_1)'/\tau_1 & 0 & 0 \\ \vdots & \vdots & \vdots \\ B(\tau_m)'/\tau_m & 0 & 0 \\ 0_{1 \times k} & 1 & 0 \\ 0_{1 \times k} & 0 & 1 \end{pmatrix}. \quad (14)$$

The covariance matrix $Q \in \mathbb{R}^{(m+2) \times (m+2)}$ has a particular structure that assumes the errors w_t are independent of \tilde{X}_t and ε_t and that $\ln \Pi_t$ and $\ln S_t$ are measured without error. The matrix has the following structure:

$$Q := \begin{pmatrix} \text{diag}(q_m^2) & 0 \\ 0 & 0 \end{pmatrix}. \quad (15)$$

If we combine (12) and (13) with the assumption that the errors are independent, we get the following joint distribution

$$\begin{pmatrix} \tilde{X}_t \\ \tilde{y}_t \end{pmatrix} \Big| \tilde{X}_{t-\Delta t} \sim \mathcal{N} \left(\begin{pmatrix} \phi + \Phi \tilde{X}_{t-\Delta t} \\ a + B(\phi + \Phi \tilde{X}_{t-\Delta t}) \end{pmatrix}; \begin{pmatrix} Q & QB' \\ BQ' & BQB' + R \end{pmatrix} \right). \quad (16)$$

However, $\tilde{X}_{t-\Delta t}$ is unknown. Our best estimation of $\tilde{X}_{t-\Delta t}$ is $\hat{X}_{t-\Delta t}$. Let $P_{t-\Delta t}$ be the covariance

matrix of the estimation error $\hat{X}_{t-\Delta t} - \tilde{X}_{t-\Delta t}$. The conditional distribution of $\hat{X}_t | \hat{X}_{t-\Delta t}$ is

$$\hat{X}_t | \hat{X}_{t-\Delta t} \sim \mathcal{N}(\phi + \Phi \hat{X}_{t-\Delta t}, P_{t|t-\Delta t}), \quad (17)$$

with $P_{t|t-\Delta t} = \Phi P_{t-\Delta t} \Phi' + Q$. Substituting this in (16) results in

$$\begin{pmatrix} \tilde{X}_t \\ \tilde{y}_t \end{pmatrix} \Big| \hat{X}_{t-\Delta t} \sim \mathcal{N} \left(\begin{pmatrix} \phi + \Phi \hat{X}_{t-\Delta t} \\ a + B(\phi + \Phi \hat{X}_{t-\Delta t}) \end{pmatrix}; \begin{pmatrix} P_{t|t-\Delta t} & P_{t|t-\Delta t} B' \\ B P_{t|t-\Delta t}' & V_t \end{pmatrix} \right), \quad (18)$$

with $V_t = B P_{t|t-\Delta t} B' + R$. We have all the information to describe the prediction and update step for the Kalman filter. Prediction is straightforward

$$\hat{X}_t = \phi + \Phi \hat{X}_{t-\Delta t}, \quad (19)$$

$$P_{t|t-\Delta t} = \Phi P_{t-\Delta t} \Phi' + Q. \quad (20)$$

The update step can be derived from the conditional density function of $\tilde{X}_t | \tilde{y}_t, \hat{X}_{t-\Delta t}$

$$\hat{X}_{t|t} = \phi + \Phi \hat{X}_{t-\Delta t} + K_t u_t, \quad (21)$$

$$P_t = P_{t|t-\Delta t} - P_{t|t-\Delta t} B' V_t^{-1} B P_{t|t-\Delta t} = (I - K_t B) P_{t|t-\Delta t}, \quad (22)$$

with $K_t = P_{t|t-\Delta t} B' V_t^{-1}$ and $u_t = \tilde{y}_t - (a + B(\phi + \Phi \hat{X}_{t-\Delta t}))$.

We can also use the Kalman smoother to estimate the optimal state given the future. The smoothed values are computed as follows:

$$\tilde{X}_{t|T} = \hat{X}_{t|t} + P_t \Phi' P_{t+\Delta t|t}^{-1} (\hat{X}_{t+\Delta t|T} - \hat{X}_{t+\Delta t|t}), \quad (23)$$

$$\tilde{P}_{t|T} = P_t - P_t \Phi' P_{t+\Delta t|t}^{-1} \Phi P_t. \quad (24)$$

4.2.1 Discretisation

To overcome the computationally intensive integrals in (12), we derive the discretised parameters using eigenvalue decomposition on $\Theta_1 = U D U^{-1}$ as in Koijen et al. (2010). The relation of the parameters of the VAR(1) process can be written as

$$\phi = U F U^{-1} \Theta_0, \quad (25)$$

$$\Phi = U \exp(D \Delta t) U^{-1}, \quad (26)$$

with F a diagonal matrix with diagonal elements $F_{ii} = \Delta t \alpha(D_{ii} \Delta t)$ and $\alpha(x) = (\exp(x) -$

1)/ x , and $\alpha(0) = 1$. The derivation of covariance matrix R is a bit more tedious. We have

$$R = UVU', \quad (27)$$

where V is a matrix with element

$$V_{ij} = [U^{-1}\Theta_2\Theta_2'(U^{-1})']_{ij} \Delta t \alpha([D_{ii} + D_{jj}]\Delta t). \quad (28)$$

4.2.2 Likelihood Function

The likelihood for Kalman filters is straightforward to derive. The joint probability density function of sequentially dependent observations can be written as $f(\tilde{y}_1, \dots, \tilde{y}_T|\theta) = f(\tilde{y}_1)f(\tilde{y}_2, \dots, \tilde{y}_T|\mathcal{I}_1) = \dots = f(\tilde{y}_1) \prod_{t=2}^T f(\tilde{y}_t|\mathcal{I}_{t-1})$, with \mathcal{I}_t all known information at time t . We observe that we can use the prediction step of the Kalman filter to obtain all the conditional probability density functions. Therefore, the distribution of $f(\tilde{y}_t|\hat{X}_{t-\Delta t})$ is a multivariate normal distribution as in (18)

$$\tilde{y}_t|\hat{X}_{t-\Delta t} \sim \mathcal{N}(a + B(\phi + \Phi\hat{X}_{t-\Delta t}), V_t). \quad (29)$$

The error, e_t , corresponding to this prediction is $e_t = \tilde{y}_t - \mathbb{E}(\tilde{y}_t|\hat{X}_{t-\Delta t})$. We can then iteratively express the log-likelihood in terms of the prediction errors as in Pelsser (2019)

$$\ln \mathcal{L}_t = -\frac{Tk}{2} \ln(2\pi) - \frac{1}{2} \ln |V_t| - \frac{1}{2} u_t' V_t^{-1} u_t, \quad (30)$$

with k the dimension and T the number of observations in the time series. We then maximise the complete log-likelihood function w.r.t. model parameters (Ψ) and ignore the constant $-\frac{Tk}{2} \ln(2\pi)$, resulting in the following maximisation problem

$$\max_{\Psi} \ln \mathcal{L} = \sum_t \ln \mathcal{L}_t = -\frac{1}{2} \sum_t \ln |V_t| - \frac{1}{2} \sum_t u_t' V_t^{-1} u_t. \quad (31)$$

4.2.3 Prior Initialisation

The Kalman filter requires an initialisation for the initial states and estimation errors. Pelsser (2019) shows superior results for a stationary initialisation, thus we opt for this option. The initial states \hat{X}_0 are set to $(\mathbb{E}[X_\infty], \ln \Pi_0, \ln S_0)$ and the initial estimation errors to

$$P_0 := \begin{pmatrix} \text{Var}[X_\infty] & 0_{2 \times 2} \\ 0_{2 \times 2} & 0_{2 \times 2} \end{pmatrix}. \quad (32)$$

The unconditional mean, $\mathbb{E}[X_\infty]$, and variance $\mathbb{V}\text{ar}[X_\infty]$ of a k -variate VAR(1) process, $X_t = c + A_1 X_{t-1} + \varepsilon_t$, are defined as

$$\mathbb{E}[X_\infty] := (I_k - A_1)^{-1}c, \quad (33)$$

$$\text{vec}(\mathbb{V}\text{ar}[X_\infty]) := (I_k - A_1 \otimes A_1)^{-1}\text{vec}(V), \quad V = \mathbb{V}\text{ar}(\varepsilon_t). \quad (34)$$

4.2.4 Restrictions

We follow the imposed restrictions on the KNW-model by the Dutch Parameter Committee 2019 (Dijsselbloem et al., 2019). The committee suggest to restrict the model such that the ultimate forward rate (UFR), unconditional expected change in inflation, and the unconditional expected return on the stock market equals predefined values. The continuously compounded ultimate forward rate is given by

$$\ln(1 + \text{UFR}) = \lim_{\tau \rightarrow \infty} \frac{A(\tau)}{\tau} = \delta_{0r} - \lambda'_0 B_\infty - \frac{1}{2} B'_\infty B_\infty, \quad B_\infty = (K + \Lambda_1)^{-1} \delta_{1r}. \quad (35)$$

The unconditional expected change in inflation and return of stocks is given by

$$\ln(1 + r_S^g) = \lim_{t \rightarrow \infty} \mathbb{E} \left[\ln \frac{S_{t+1}}{S_t} \right] = \delta_{0r} + \eta_s - \frac{1}{2} \sigma'_S \sigma_S, \quad (36)$$

$$\ln(1 + r_\Pi^g) = \lim_{t \rightarrow \infty} \mathbb{E} \left[\ln \frac{\Pi_{t+1}}{\Pi_t} \right] = \delta_{0\pi} - \frac{1}{2} \sigma'_\Pi \sigma_\Pi. \quad (37)$$

Committee Parameters suggest to set the UFR to 2.1%, r_S^g to 5.6% and r_Π^g to 1.9%. This results in the following constraints:

$$\delta_{0r} = \ln(1.021) + \lambda'_0 B_\infty + \frac{1}{2} B'_\infty B_\infty, \quad (38)$$

$$\eta_s = \ln(1.056) - \delta_{0r} + \frac{1}{2} \sigma'_S \sigma_S, \quad (39)$$

$$\delta_{0\pi} = \ln(1.019) + \frac{1}{2} \sigma'_\Pi \sigma_\Pi. \quad (40)$$

The degrees of freedom of the model decrease by three. This model will be referred to as the restricted KNW-model.

4.3 Parameter Uncertainty

Chen et al. (2019) simulate the economy using point estimates of the KNW-model. We suggest that the uncertainty of the parameters should be considered when simulating the economy.

Under regularity assumptions the maximum likelihood estimate (MLE) of the Kalman filter are consistent and asymptotically normal with a covariance matrix equal to the negative inverse matrix of the (Fisher) information matrix, $\mathcal{F}_{\mathcal{L}}$ (Caines, 2018). The assumptions require that the model is identifiable and the true parameter values are not at the boundary of parameter space. The information matrix contains the second-order partial derivatives of the log-likelihood function \mathcal{L} w.r.t. all model parameters, thus mathematically³

$$\mathcal{F}_{\mathcal{L}} = \frac{\partial^2 \ln \mathcal{L}}{\partial \theta^2} = \left(\begin{array}{ccc} \frac{\partial^2 \ln \mathcal{L}}{\partial \delta_r \partial \delta_r} & \cdots & \frac{\partial^2 \ln \mathcal{L}}{\partial \delta_r \partial h} \\ \vdots & \ddots & \\ \frac{\partial^2 \ln \mathcal{L}}{\partial h \partial \delta_r} & \cdots & \frac{\partial^2 \ln \mathcal{L}}{\partial h \partial h} \end{array} \right)_{\theta = \hat{\theta}_{MLE}}, \quad (41)$$

with θ denoting all model parameters. Let $\hat{\theta}_{MLE}$ be the maximum likelihood estimate of the Kalman filter. We then can draw a new parameter set i by taking draws from the following distribution $\theta_{(i)} \sim \mathcal{N}(\hat{\theta}_{MLE}, -\mathcal{F}_{\mathcal{L}}^{-1})$. We obtain a normally distributed set of parameters around $\hat{\theta}_{MLE}$ with covariance $-\mathcal{F}_{\mathcal{L}}^{-1}$.

One of the issues of sampling from a distribution is that implicit parameters restrictions are no longer enforced. To make sure our simulations of states are stationary under measure \mathbb{Q} , we omit all draws where the eigenvalues of K or $M = K + \Lambda$ are non-negative or not real.

Another method to approximate the standard errors is by means of bootstrapping. By generating new data sets using the initially estimated parameters and re-estimating the model, we can create a distribution of parameters. However, due to the high number of parameters in the KNW-model this method is infeasible. Since we have 29 parameters in the KNW-model and 26 parameters in the restricted KNW-model, the number of bootstraps needs to be very large. This requires too much computation time.

4.4 Pension Fund

Asset liability management (ALM) analysis assess the risk that is taken by a financial institution through modelling its assets and liabilities. In this section we describe how assets and liabilities of our pension fund are modelled. The liabilities, L_t , of a pension fund consist of the outstanding claims of its participants. This includes current claims and discounted future claims. The assets of the pension fund are denoted by A_t and are obtained via participant's contributions and financial returns on the assets. The financial well-being of a pension fund is described by the coverage ratio (CR). The ratio describes the ratio of assets to liabilities ($\frac{A_t}{L_t}$). For example, a

³For readability purposes we do not fully write out all subscripts of the parameters, therefore each partial derivative is a block-matrix.

coverage ratio of 1 means the pension funds has exactly enough assets to pay for its outstanding claims. Whenever a pension fund reaches a coverage ratio greater than 1, it can increase the benefits for its members, and vice versa. Altering the pension benefits is called indexation, denoted by I_t . The indexation rules are defined as follows

$$I_t = \begin{cases} \frac{A_t}{0.9L_t} - 1 & \text{if } CR_t < 90\% \\ \frac{A_t - L_t}{(x-1)A_t + L_t} & \text{if } 90\% \leq CR_t \leq 120\% \\ \frac{A_t - L_t}{(x/2-1)A_t + L_t} & \text{if } CR_t > 120\%. \end{cases} \quad (42)$$

Financial shocks do not have to be included in the indexation immediately. To smooth out financial shocks over time, a spreading factor x is used. It spreads out the financial shocks over x years. It is set to ten years in our study. If the coverage ratio reaches a value between 90% and 120%, around 1/10th of the excess/shortage is divided. If the coverage ratio is above 120%, the indexation is performed twice as quickly, thus 1/5th of the excess is divided. There are two backstops present in this system. If the coverage ratio drops below 90%, one backstop is enacted where pension benefits are immediately decreased such that the coverage ratio is set back to 90%. The second backstop is carried out when the coverage ratio is below a 100% for five consecutive years. In this case the ratio is set back to 100% with an indexation of $I_t = \frac{A_t}{L_t} - 1$. The indexation for the backstops is spread over a period of 10 years.

The assets of a pension fund are highly dependent on the performance of their investment portfolio. A fund's portfolio consists of a mix between stocks and bonds. The return of a fund's portfolio depends on their allocation, so

$$R_t = 1 + x_1 r_t^1 + x_2 r_t^2 + (1 - x_1 - x_2) r_t, \quad (43)$$

with x_1 and x_2 the percentage invested in stocks and cash-flow matching bonds respectively. The returns of the stock index is denoted by r_t^1 . r_t^2 is the return on the bond portfolio. Finally, a fraction $1 - x_1 - x_2$ is invested in the instantaneous nominal interest rate (r_t). Note that the fund can borrow money to invest in either stocks or bonds, and therefore the last fraction $1 - x_1 - x_2$ can be negative. Given the return on the portfolio the assets develop as

$$A_{t+1} = R_{t+1}(A_t + Inc_t - Exp_t), \quad (44)$$

with Inc_t the income from contributions of participants and Exp_t the expenditures related to paying off claims at time t .

To find out the exact effect of parameter uncertainty, we simulate the pension fund and its participants similar to Chen et al. (2019). Every year a single person joins the system and represents a generation (cohort). We make some assumptions about each agent's life. An agent starts working at 25 and retires at 65. During this period (T_W), he contributes 20% of his salary towards his pension. An agent benefits from its pension for 20 years and passes away at the age of 85 years. This period is denoted by T_P . At the start of each simulation wages are set to 25,000 euros and grow with the price index. The starting value of assets is equal to its liabilities, thus a CR of 100%.

The pension claims of cohorts $j \in \{t - T_W - T_P, \dots, t - 1\}$ result in cash flows in $\tau \in \{\max(0, j - t + T_W + 1), \dots, j - t + T_W + T_P\}$ periods. To keep track of the claims for each cohort we define a matrix Q . Let $Q \in \mathbb{R}^{(T_W+T_P) \times (T_W+T_P)}$ be a matrix of zeros and ones. Column j represent whether cohort $k = t - j$ will receive a payment in $i - 1$ periods. Then for each element $q_{i,j} \in Q$ we get

$$q_{i,j} = \begin{cases} 1 & \text{if } i + j \in \{T_W + 2, \dots, T_W + T_P + 1\} \\ 0 & \text{if } i + j \notin \{T_W + 2, \dots, T_W + T_P + 1\}. \end{cases}$$

In order to track the pension claims at each time t , we define a matrix $B_t \in \mathbb{R}^{(T_W+T_P) \times (T_W+T_P)}$. Again, column j represent cohort $k = t - j$ but with the nominal cash flow the cohort will receive in $i - 1$ years. Thus, each row i represent what the pension fund has to pay in $i - 1$ years to each cohort. As we deal with future payoffs, we need a discount factor, $DF_t(\tau)$, to discount future payoffs. We use the price of a zero-coupon bond with maturity τ as the discount factor. The liabilities can then be computed as

$$L_t = \sum_{j=t-T_W-T_P}^{t-1} \sum_{i=1}^{T_W+T_P} (DF_t(i-1) q_{i,t-j} (B_t)_{i,t-j}). \quad (45)$$

4.5 Risk Allocation

To not distribute risk uniformly across different age groups, we make use of an adjustment factor. The adjustment factor $af_{j,t}$ alters the indexation for age group j at time t . The exact change in benefits for each cohort j is given by $v_{j,t} \in \mathbb{R}^{T_W+T_P}$, where

$$v_{j,t} = \iota \xi_t af_{j,t}, \quad (46)$$

with $\iota \in \mathbf{1}^{(T_W+T_P)}$, a vector of ones, and ξ_t a scaling factor. The relative change in pension claims that are due in i years is given by the i -th element of $v_{j,t}$. The scaling factor ξ_t is chosen

such that the liabilities scale with the indexation, thus

$$(1 + I_t)L_t = \sum_{j=t-T_W-T_P}^{t-1} \sum_{i=1}^{T_W+T_P} (DF_t(i-1) q_{i,t-j}(B_t)_{i,t-j}(1 + (v_{j,t})_i)).$$

In the following sections, we introduce the three different risk allocations as in Chen et al. (2019). All three risk allocations allocate more risk to younger generations than older generations. The exact form of the different adjustment factors are shown in Section 5.3.1. For the base case, no age-dependent risk allocation is present, and thus has an adjustment factor of one for all ages.

4.5.1 3-2-1 Adjustment Rule

Dillingh et al. (2018) propose an age-dependent allocation rule based on a 3-2-1 adjustment rule. We assume that people contribute for 40 years to their pension and benefit for 25 years of the payments. The youngest 30 generations have an adjustment factor of three, the middle 10 generations a factor of two, and all pensioners an adjustment factor of one. The adjustment factor is defined as follows:

$$af_{j,t} = \begin{cases} 3 & \text{if } t-j \in \{1, \dots, T_W - 10\} \\ 2 & \text{if } t-j \in \{T_W - 9, \dots, T_W\} \\ 1 & \text{if } t-j \in \{T_W + 1, \dots, T_W + T_P\}. \end{cases}$$

4.5.2 Uniform Adjustment to Achievable Pension

Rather than using age as a proxy for built up pension, we can also directly use the built up pension. Muns and Werker (2019) suggests to allocate risk by uniformly adjusting to the achievable pensions. This means that during every moment in their lifetime the adjustment to their pension is proportional to their built up pension. To describe this mathematically, we define $W_{j,t}$ as the built up pension for cohort j at time t and $H_{j,t}$ as the expected pension claims. The adjustment factor is computed as a fraction of the built up pension plus the expected pension claims divided by the built up pension,

$$af_{j,t} = \frac{W_{j,t} + H_{j,t}}{W_{j,t}}. \tag{47}$$

The variables $W_{j,t}$ and $H_{j,t}$ are computed as follows:

$$W_{j,t} = \sum_{i=1}^{T_W+T_P} DF_t(i-1) q_{i,t-j} (B_t)_{i,t-j}, \quad (48)$$

$$H_{j,t} = \sum_{\tau=1}^{T_W+j-t-1} DF_t(\tau) \tilde{w}_{t+\tau}, \quad (49)$$

with $DF_t(\tau)$ the discount factor for τ years computed at time t . Retirees have no more expected pension claims ($H_{j,t} = 0$), and thus an adjustment factor equal to one. We assume the wages will grow with the price index, therefore the expected future salary in τ years will be

$$\tilde{w}_{t+\tau} = \Pi_t \exp\left\{\tau\delta_{0\pi} + \delta'_{1\pi} X_t \sum_{s=1}^{\tau} \exp(-sK)\right\}. \quad (50)$$

4.5.3 Optimisation over the Life Cycle

Finally, we present the third adjustment factor. Rather than setting a fixed adjustment factor or using the built up pension directly, we use a parametric adjustment factor. This gives us the opportunity to create a flexible adjustment factor. We then optimise both over the parameters as well as the portfolio allocation x_1 and x_2 . The function has the form as introduced in Chen et al. (2019) and contains three parameters β_1, β_2 and β_3 . The function is defined as

$$f(k) = \exp\left\{\beta_1(T_W + T_P - k) + \beta_2 \max\{0, T_W - k\} + \beta_3 \max\{0, T_W - k\}^2\right\}, \quad (51)$$

where k represents the number of years a cohort has worked. The adjustment factor is then defined as $af_{(t-k),t} = f(k)$.

4.6 Measuring Welfare

To quantify welfare gains or losses over age-dependent risk allocation, we need a measure for welfare. A utility framework is used. People have different preferences for risk and can be either risk averse, risk neutral or risk seeking. Risk aversion indicates that people feel diminishing rewards as risk increases and therefore need to be compensated more for taking additional risk. Risk neutrality means that people are indifferent between risk levels, and risk seeking people reward additional risk. Measures for absolute and relative risk aversion have been introduced by Pratt (1964) and Arrow (1965). A common measure in literature is the constant relative risk aversion (CRRA), with utility function

$$u(x) = \frac{x^{1-\gamma}}{(1-\gamma)} \quad (52)$$

and γ denotes the risk aversion parameter. In our case, similar to Chen et al. (2019), we will use a parameter value of $\gamma = 5$. This value is widely used in the literature as the standard risk aversion parameter. The total utility of cohort j , during their pension, in simulation i is equal to

$$U_{j,i} = \sum_{t=j+T_W+1}^{j+T_W+T_P} \rho^{t-j-T_W-1} u\left(\frac{(B_t)_{1,t-j}}{\Pi_t}\right),$$

where ρ is a subjective discount rate, set to the steady-state instantaneous interest rate. The expected utility of cohort j is the average over $i = 1, \dots, N$ simulations

$$\bar{U}_j = \mathbb{E}(U_j) = \frac{1}{N} \sum_{i=1}^N U_{j,i}. \quad (53)$$

We can write welfare as the certainty equivalent consumption (CEC) so that the CEC for cohort j is equal to

$$CEC_j = \left(\bar{U}_j \frac{1-\gamma}{\sum_{t=1}^{T_P} \rho^t}\right)^{\frac{1}{1-\gamma}}, \quad (54)$$

which we can rewrite to express utility as a function of CEC:

$$\bar{U}_j = \sum_{t=1}^{T_P} \rho^t u(CEC_j). \quad (55)$$

The total welfare (TW) is a sum of discounted expected utilities starting after the burn-in period k . Using some rules for power series, we obtain

$$\begin{aligned} TW &= \sum_{j=k}^{\infty} \rho^j \bar{U}_{j-T_W} = \sum_{j=k}^{\infty} \rho^j \sum_{t=1}^{T_P} \rho^t u(CEC_{j-T_W}) \\ &= \frac{\rho^k}{1-\rho} \sum_{t=1}^{T_P} \rho^t u(CEC) = \frac{\rho^{k+1}}{1-\rho} \frac{1-\rho^{T_P}}{1-\rho} u(CEC). \end{aligned} \quad (56)$$

Due to computational limitations, we only simulate 600 years equivalent to Chen et al. (2019). Increasing the number of years is not necessary as the effect after 600 years is almost negligible due to the discount factor ρ . We can rewrite CEC as a function of TW

$$CEC = \left(\frac{TW(1-\rho)^2(1-\gamma)}{(1-\rho^{T_P})\rho^{k+1}}\right)^{1/(1-\gamma)}. \quad (57)$$

By means of optimisation we can find the optimal investment strategy to maximise total welfare. We want to find x_1 and x_2 so that CEC is maximised, thus $\max_{x_1, x_2} CEC$. For the method described in Section 4.5.3, we also need to optimise over the parameters $\beta = (\beta_1, \beta_2, \beta_3)$

in (51). In this case our problem is defined as

$$\max_{x_1, x_2, \beta} CEC. \quad (58)$$

Due to computational limitations we cannot optimise over all the 10,000 scenarios. Therefore, we only use 1,000 scenarios to find the optimal parameters. Finally, we compute welfare gains or losses as the percentage change of the CEC of an allocation method over the CEC of the uniform adjustment rule.

4.6.1 Standard Error

To approximate the distribution of the welfare gains and losses, we use a bootstrap method. We perform a bootstrap by taking a random sample of size N of the utilities U_i for two different allocation methods. Both methods take the exact same economies. We compute the average welfare gain or loss over two using the CEC as in (57). We repeat this bootstrap 10,000 times to obtain our bootstrap distribution.

4.7 CEC Analysis

To better understand what factors affect welfare, we perform a regression analysis. For each simulation we take the average CEC across all cohorts and regress the CEC on a set of independent variables. We consider the average 10 year bond price, the average short-rate, the standard deviation of the short-rate, the average stock return and the standard deviation of the stock return within a simulation. Formally,

$$CEC_i = \beta_0 + \beta_1 X_{1i} + \beta_2 X_{2i} + \dots + \beta_k X_{ki} + \varepsilon_i, \quad i \in \{1, \dots, N\}, \quad (59)$$

with X_{ji} the j -th independent variable for simulation i , k the number of independent variables and N the number of simulations.

5 Results

In this section, we describe the results of parameter estimates of the Kalman filter in Section 5.1. Thereafter, we present descriptive statistics of the generated scenario sets in 5.2. The results of the pension fund simulation can be found in Section 5.3.

Param.	Unrestricted		Restricted		Pelsser (Restricted)	
	Coefficient	S.E.	Coefficient	S.E.	Coefficient	S.E.
$\delta_{0\pi}$	0.0194	0.0000	0.0188		0.0188	
$\delta_{1\pi,1}$	-0.0018	0.0000	-0.0014	0.0000	-0.0023	0.0015
$\delta_{1\pi,2}$	-0.0009	0.0000	-0.0009	0.0000	0.0003	0.0011
δ_{0r}	0.0212	0.0003	0.0193		0.0211	
$\delta_{1r,1}$	-0.0056	0.0000	-0.0054	0.0000	-0.0077	0.0005
$\delta_{1r,2}$	-0.0009	0.0000	-0.0008	0.0000	0.0010	0.0023
K_{11}	0.0312	0.0017	0.0421	0.0047	0.0386	0.0749
K_{22}	1.1056	0.0965	0.4312	0.0651	0.2629	0.1783
K_{21}	0.4493	0.1357	0.4195	0.0314	0.3774	0.2158
$\sigma_{\Pi,1}$	-0.0016	0.0000	-0.0015	0.0000	-0.0007	0.0005
$\sigma_{\Pi,2}$	0.0017	0.0000	0.0009	0.0000	0.0008	0.0004
$\sigma_{\Pi,3}$	0.0061	0.0000	0.0061	0.0000	0.0055	0.0003
$\sigma_{S,1}$	-0.0431	0.0004	-0.0396	0.0002	-0.0549	0.0104
$\sigma_{S,2}$	0.0595	0.0004	0.0310	0.0003	0.0044	0.0183
$\sigma_{S,3}$	0.0056	0.0001	0.0045	0.0001	0.0002	0.0032
$\sigma_{S,4}$	0.1428	0.0000	0.1436	0.0000	0.1305	0.0064
η_S	0.0629	0.0015	0.0467		0.0434	
$\lambda_{0,1}$	0.5581	0.0134	0.6244	0.0458	0.6377	0.1675
$\lambda_{0,2}$	-0.1284	0.0389	-0.1140	0.0603	-0.0745	0.2054
$\Lambda_{1,1}$	0.2593	0.0602	0.2236	0.0069	0.1717	0.0626
$\Lambda_{1,2}$	0.8569	0.0098	0.3406	0.0104	0.1875	0.0602
$\Lambda_{2,1}$	-0.4419	0.1977	-0.4268	0.0676	-0.3887	0.2485
$\Lambda_{2,2}$	-1.0670	0.1252	-0.4154	0.0254	-0.2429	0.1516
h_1	0.0000	0.0000	0.0000	0.0000	0.0032	0.0002
h_5	0.0014	0.0000	0.0017	0.0000	0.0007	0.0001
h_{10}	0.0005	0.0000	0.0006	0.0000	0.0004	0.0000
h_{15}	0.0001	0.0000	0.0005	0.0000	0.0000	0.0001
h_{20}	0.0008	0.0000	0.0009	0.0000	0.0011	0.0001
h_{30}	0.0024	0.0000	0.0029	0.0000	0.0002	0.0002
$\log \mathcal{L}$	9653.35		9508.76		***	
R^2	0.9936		0.9955		***	
min.ev(K)	0.0312		0.0421		0.0386	
min.ev(M)	0.0156		0.0261		0.0319	
Π -return	0.0193		0.0188		***	
S-return	0.0711		0.0545		***	

Table 1: Parameter estimates. This table shows the results of both the unrestricted and restricted KNW-model estimated with data ranging from January 2004 to September 2021. The most right column shows the parameters estimated by Pelsser (2019). Note that the data used by us and Pelsser (2019) to estimate the parameters differ. In the bottom of the table $\log \mathcal{L}$ denotes the log-likelihood and min.ev the smallest eigenvalue of a matrix. The *** denotes unavailable or non-relevant data. R^2 is based on the smoothed states by the Kalman smoother.

5.1 Parameter Estimates

Table 1 shows the estimated parameters of the restricted and unrestricted KNW-model. The standard errors of the parameters are computed using the second-order derivative of the negative log-likelihood function w.r.t. each parameter. These values can be found in the diagonal of the covariance matrix $-\mathcal{F}_{\mathcal{L}}^{-1}$, as described in (41). If we compare the two different models we notice a lower log-likelihood for the restricted models. This is to be expected as this model has less freedom in its choice of parameters. The log-likelihood of the restricted model drops by $9653.35 - 9508.76 = 144.59$. A difference is noticeable in the matrices K and Λ . K_{22} especially gets shrunk by a noticeable amount from 1.1056 to 0.4312. The standard errors of the matrix K also drop noticeably for K_{22} and K_{21} , indicating a better fit for the K matrix. We observe the same shrinkage in the matrix Λ , where their absolute values as well as standard errors decrease notably. The largest parameters in these models get shrunk, which results in larger minimum eigenvalues. Negative eigenvalues indicate a non-stationary process which means that inflation, bond prices and stock prices diverge as time increases. Non-negative eigenvalues are beneficial for economic simulations as they create more realistic economic scenarios. If we follow the model restrictions of the Dutch Parameter Committee 2019, the equity risk premium goes down from 6.29% to 4.67%. We cannot directly compare the parameter estimates by Pelsser since the data used for calibration differ. However, we can still observe that the parameters are relatively close to our estimates. An odd observation is that the standard errors differ a lot. The reason for this remains unknown and is likely due to different numerical approximation techniques for the Hessian. It is interesting to compare the estimated stock return and inflation to our data set. The annual historic stock return in our data set is 6.11%, which falls somewhere in between the unrestricted and restricted model. The inflation in our data is at 1.58%, which is closer to estimates of the restricted model.

5.2 Economic Scenarios

This section shows some descriptive statistics of the economic scenario sets. We check how parameter uncertainty affects the generated scenarios and its descriptive statistics. Table 2 shows that the first three moments are relatively similar in both scenario sets. However, the fourth moment, kurtosis, increases for the short-rate and inflation. This means that the distribution has fatter tails and thus extreme values are more likely to occur. In the following section we will show how this impacts the welfare changes for different risk allocations.

	Mean	Std. Dev.	Skewness	Kurtosis
<i>Scenario set 1 (without S.E.)</i>				
Stock-index	6.55%	15.35%	0.00	3.00
Short-rate	1.88%	1.86%	0.02	3.01
Inflation	1.87%	0.81%	0.01	3.00
<i>Scenario set 2 (with S.E.)</i>				
Stock-index	6.58%	15.46%	0.00	3.03
Short-rate	1.94%	1.79%	0.02	3.44
Inflation	1.87%	0.82%	0.00	3.34

Table 2: Descriptive statistics scenario sets. This table shows the descriptive statistics of the two scenario sets. We describe the first four moments (mean, standard deviation, skewness and kurtosis).

5.3 Pension Fund Simulation

Table 3 shows the welfare gains of different risk allocation methods in comparison to the base uniform distribution of risk for both simulations with and without standard errors. We find results in line with earlier research (Chen et al., 2019; Darmoutomo et al., 2020). For the simulation without standard errors, the 3-2-1 distribution rule is the only allocation method that results in a welfare loss in comparison to the benchmark uniform distribution of risk method. The risk distribution methods of uniform adjustment in achievable pension and optimisation over

Method	Welfare Increase (%)	S.E. (%)
<i>Simulation without standard errors</i>		
3-2-1 distribution rule	-1.79***	0.53
Uniform adjustment in achievable pension	2.59***	0.70
Optimisation over the life cycle	3.08***	0.24
<i>Simulation with standard errors</i>		
3-2-1 distribution rule	-2.10***	0.77
Uniform adjustment in achievable pension	0.93	1.99
Optimisation over the life cycle	-0.46	1.74

Table 3: Welfare gains over different risk allocation methods. This table shows increase in welfare measured by average certainty equivalent in consumption (CEC) over different risk allocation methods. * denotes significance level at 10%, ** at 5%, and *** at 1%.

the life cycle show an average welfare gain of 2.59% and 3.08% respectively. We find significant welfare gains at the 1% significance level for all methods. For the simulation with standard errors the results differ. In this section the 3-2-1 distribution rule and the optimisation over the life cycle lead to welfare losses compared to the base model of 2.10% and 0.46% respectively. The uniform adjustment in achievable pension rule gives us an average welfare gain of 0.93%. Furthermore, we find that not all results are significant anymore at even the 10% significance

level. Only the 3-2-1 distribution rule’s welfare loss is significant at the 1% significant level.

Method	x_1 (%)	x_2 (%)
<i>Simulation without standard errors</i>		
Base uniform	48.7	100.0
3-2-1 distribution rule	40.8	100.0
Uniform adjustment in achievable pension	40.5	100.0
Optimisation over the life cycle	48.7	100.0
<i>Simulation with standard errors</i>		
Base uniform	47.65	99.95
3-2-1 distribution rule	37.92	100.0
Uniform adjustment in achievable pension	46.55	100.0
Optimisation over the life cycle	55.47	99.09

Table 4: Allocation over different risk allocation methods. This table shows the allocation in equity (x_1) and the interest rate hedges (x_2) over different risk allocation methods. The allocations are obtained using 1000 simulations.

Table 4 shows the allocation into equity (x_1) and interest rate hedges (x_2). For the simulation without standard errors, we find relatively similar results for all methods with weights in equity ranging from 40% to 50%. For the simulation with standard errors included, we observe a broader range of allocations in equity, ranging from 37% to 55%. In terms of interest rate hedges both simulations result in a value close to or equal to 100%. For all methods the optimal strategy is to (almost) hedge all of the interest rate risk. We find that all positions are leveraged as $x_1 + x_2 > 100\%$. This means part of the investments is financed by going short in the short rate. This is expected behaviour as the short rate has been close to zero or even negative in recent years, making short positions relatively cheap.

5.3.1 Adjustment Factors

Figure 3 shows the adjustment factors for both simulations. When we do not consider the standard errors in our simulation, we observe a relatively flat adjustment factor curve for the optimisation over the life cycle. When people join the pension system they have an adjustment factor of around 3.5 times than that of a retired person. This factor slowly decays to the age of around 65, where it reaches an adjustment factor of one. The uniform to achievable pension is much more convex, and has a very high adjustment factor at the start. On the right of Figure 3, we find a similar shape for the uniform to achievable pension, however the optimisation over the life cycle shows almost the same steepness as the uniform adjustment in achievable pension. An interesting observation is the dip for people aged between 40 and 65. It seems that this function can only obtain this steep exponential decay by going slightly below the adjustment factor one

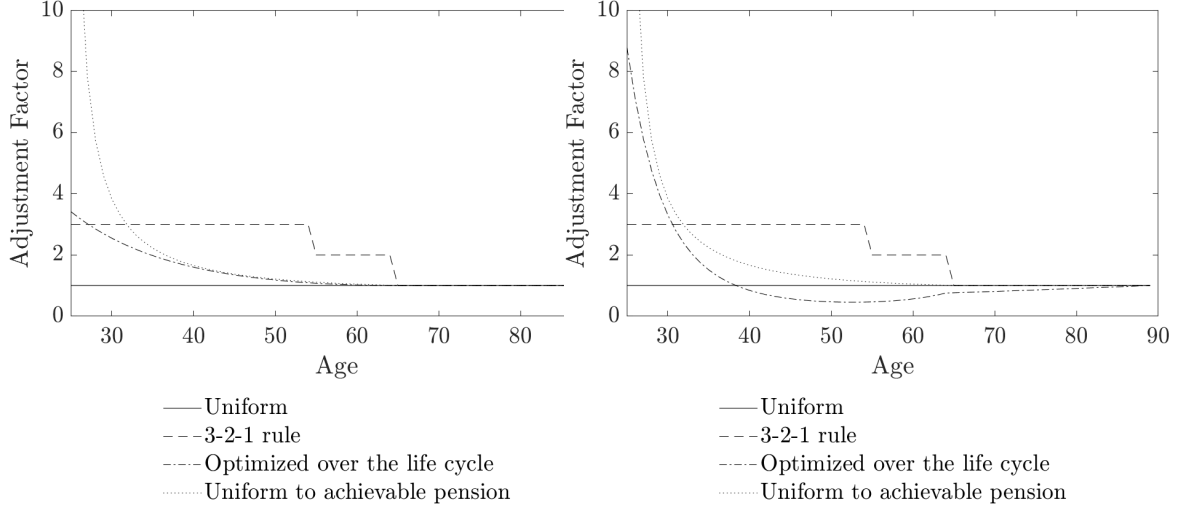


Figure 3: Adjustment factors. The figure on the left shows the adjustment factors for the simulation without considering standard errors. The figure on the right shows the adjustment factors for the simulation with standard errors.

at some cohorts.

5.3.2 Robustness Checks

The results for the robustness checks for both types of simulations are shown in Table 5. The table shows varying the risk aversion parameters γ of the CRRA utility function. We also vary the spreading factor x from 1 to 9 years. The risk parameter $\gamma = 3$ denotes a lower risk aversion, and $\gamma = 7$ a higher one than the default value of $\gamma = 5$. In Panel A, we have the results for the simulation without standard errors. For $\gamma = 3$, we find higher welfare gains for all methods in comparison to $\gamma = 5$. This is as expected as a lower risk aversion leads to higher risk taken by the pension fund. The potential benefit of efficient risk allocation leads thus to higher welfare gains. In contrary, a higher risk risk aversion leads to less benefit in utility when risk is distributed more evenly. Therefore, we find lower welfare gains and even welfare losses. We also find a positive correlation between the welfare gains and the spreading factor. We observe that a higher spreading factor results to higher welfare gains. This is conform expectations as negative economic shocks are spread out over several generations. Due to the non-linearity of the CRRA function, this leads to smaller negative utilities.

Panel B shows the results for simulation with the standard errors considered. Again, we find similar results when changing the risk parameter. The lower risk aversion ($\gamma = 3$) leads to higher welfare gains compared to $\gamma = 5$. We find a welfare loss for the 3-2-1 distribution rule of -1.99% , and 9.71% and 18.58% for the uniform adjustment in achievable pension and optimisation over the life cycle respectively. The welfare gain of the 3-2-1 distribution rule is significant at the 10% significance level, the uniform adjustment in achievable pension and optimisation over the life

Method	Welfare Gain (%)	S.E. (%)	x_1 (%)	x_2 (%)	
Panel A: Simulation without standard errors					
$\gamma = 3$	3-2-1 distribution rule	-1.39***	0.36	78.15	99.92
	Unif. adj. in ach. pension	9.42***	0.50	60.39	100.00
	Opt. over the life cycle	10.24***	3.66	75.20	100.00

$\gamma = 7$	3-2-1 distribution rule	-2.84***	0.77	27.58	100.00
	Unif. adj. in ach. pension	-2.35	1.99	23.74	100.00
	Opt. over the life cycle	0.22	1.74	34.25	100.00

$x = 1$		-1.67***	0.54	46.08	100.00
$x = 2$		-1.08**	0.57	44.87	100.00
$x = 3$		-0.41	0.59	43.50	100.00
$x = 4$		0.15	0.59	43.31	99.98
$x = 5$	Unif. adj. in ach. pension	0.58	0.62	42.71	100.00
$x = 6$		1.02	0.65	42.88	100.00
$x = 7$		1.39**	0.66	41.66	100.00
$x = 8$		1.78***	0.67	41.26	100.00
$x = 9$		2.17***	0.69	40.89	100.00

Panel B: Simulation with standard errors					
$\gamma = 3$	3-2-1 distribution rule	-1.99*	0.38	53.17	99.98
	Unif. adj. in ach. pension	9.71***	0.49	68.16	100.0
	Opt. over the life cycle	18.58***	0.81	70.01	99.00

$\gamma = 7$	3-2-1 distribution rule	-4.30***	1.54	32.97	90.39
	Unif. adj. in ach. pension	-10.09**	4.36	39.09	99.98
	Opt. over the life cycle	-6.70**	3.20	47.78	99.28

$x = 1$		-0.06	1.66	50.26	100.00
$x = 2$		-0.25	1.66	51.51	100.00
$x = 3$		-0.04	1.71	50.87	99.95
$x = 4$		-0.06	1.79	50.00	100.00
$x = 5$	Unif. adj. in ach. pension	0.00	1.77	49.66	100.00
$x = 6$		0.21	1.77	49.16	99.96
$x = 7$		0.22	1.87	48.25	99.97
$x = 8$		0.65	1.95	47.56	99.98
$x = 9$		1.04	1.97	46.17	99.99

Table 5: Robustness checks for welfare gains. This table shows the welfare gains and losses measured by average certainty equivalent in consumption (CEC) using different risk allocation methods. The welfare increases are compared against the benchmark allocation, the uniform adjustment rule, in terms of CEC. For the varying spreading factor, x , the benchmark uniform adjustment rule always has $x = 10$, to be able to compare the welfare gains across different values of x . Welfare is measured over 10,000 simulations. Standard errors are obtained via 10,000 bootstrap repetitions. The superscript * denotes the significance level at 10%, ** at 5%, and *** at 1%.

cycle at the 1% level. Again, similar to Panel A, we find higher welfare losses for $\gamma = 7$. We find that when we take standard errors into account all methods lead to welfare losses. The losses

range from -4.30% to -10.09% across the different allocation rules. For the different spreading factors x , we find similar results to the case where we do not take standard errors into account. However, the welfare losses and gains are closer to zero and none of the values are significantly different from zero at the 10% significance level.

5.3.3 Effect of Factors

Variable	Uniform distribution rule	3-2-1 distribution rule	Unif. adj. in achiev. pension	Opt. over life cycle
<i>Scenario set 1 (without S.E.)</i>				
Constant	0.82***	0.87***	0.95***	0.94***
Avg. 10Y bond price	-0.73***	-0.79***	-0.86***	-0.85***
Avg. short-rate	-5.42***	-6.05***	-6.77***	-7.15***
Std. short-rate	-1.84***	-2.17***	-2.48***	-2.45***
Avg. stock return	5.53***	6.08***	6.25***	6.97***
Std. stock return	-1.53***	-1.70***	-1.73***	-1.93***
R^2	0.3203	0.3133	0.3260	0.3228
<i>Scenario set 2 (with S.E.)</i>				
Constant	1.06***	1.10***	1.27***	1.24***
Avg. 10Y bond price	-1.10***	-1.17***	-1.35***	-1.30***
Avg. short-rate	-6.35***	-6.44***	-9.47***	-9.49***
Std. short-rate	-0.19	-0.16	-0.19	-0.46
Avg. stock return	4.74***	4.76***	7.23***	7.59***
Std. stock return	-1.01***	-0.94***	-1.51***	-1.79***
R^2	0.3495	0.3491	0.3362	0.3360

Table 6: Regression results. This table report the coefficients of several factor regressed on the certainty equivalent of consumption. The risk aversion parameter γ is equal to 5 for both scenario sets. All values are scaled down by $1e-5$. *, **, and *** denote the 10%, 5%, and 1% significance level respectively.

We briefly analyse the effect of certain independent variables on the CEC by means of regression. Table 6 shows the effect of each variable on CEC. The independent variables are characteristics of the scenario set. First, the signs of the parameter estimates show that an increase in the 10-year bond price results in a lower CEC. The same holds for an increase in average short-rate, standard deviation of the short-rate and an increase in volatility in the stock market. Only the standard deviation of the short-rate has no significant effect on the CEC. Another interesting observation is that the magnitude of the parameters increase as the adjustment factor function gets more flexible. The uniform adjustment in achievable pension and optimisation over the life cycle are the most flexible functions and have the largest magnitude in comparison to the other two allocation rules. The 3-2-1 distribution rule however, is fairly

similar to the uniform distribution rule in terms of magnitude. The results are intuitive. Higher bond prices heavily effect pension funds liabilities as future payoffs are more expensive. More volatility causes unstable growth of the assets. Higher stock returns however have a clearly positive effect on the fund. The difference between the two scenario sets is that the standard deviation of the shock-rate is significantly different from zero at the 1% level for scenario set 1. The exact reason for this is unclear, but again the effect is negative. This shows that uncertainty in the short-rate has a negative effect on the CEC.

6 Discussion

In this section we take a deeper look into the obtained results and discuss the potential problems and limitations of this research.

First, we discuss the results of the KNW-model estimates. The parameters estimated by the Kalman filter show similar results to the parameters estimated by Pelsser (2019). By restricting the UFR, the unconditional expected change in inflation and return, we got improved estimates for the parameters K and Λ . The question remains whether the restrictions are reasonable. A yearly inflation growth of close to but under 2% has been the policy by the European Central Bank for a long period and can be supported by our data. In the unconstrained KNW-model we find that the risk premium η_S was estimated to be higher. This is supported by the data, as the index grew a lot in the recent years. However, a slightly lower equity risk premium might be desirable. The economic data we used does not capture too many recessions, however when we take a longer horizon into account, average stock index growth has been lower. We can see the restrictions as a desired or long run equilibrium for the economy. Especially in our case where the parameters are used to simulate economic scenarios. The same argument can be made for the UFR. Even though the interest rates are very low at the moment, we do not expect them to stay low in the long run. Therefore, taking the restricted KNW-model can be a nice balance between capturing the dynamics of the economy as well as putting a prior on long run equilibrium values of the economy.

It is impossible to simulate a real world pension fund and population, therefore we work with a simplified model of reality. Our model does not take the ageing society nor population growth into account, assumes wages grow perfectly with inflation and assumes perfect liquidity of the bond market. The effect of a greying population leads to a lower coverage ratio, assuming other variables stay the same. Further research can perform a stress-test to quantify the effect on welfare by a greying population. Moreover, we assume that we can perfectly hedge all interest rate risk by buying cash flow matching bonds. However, in reality bonds and derivatives are not

widely available for maturities above 30 years. In practice it is also possible to hedge liabilities with different maturities with different amounts, e.g. hedging short maturities more than long term or vice versa.

We find that incorporating parameter uncertainty into the economic scenario generator leads to different inference than excluding parameter uncertainty. We show that multiple factors affect the CEC. The distribution around inflation and interest rates is more fat-tailed when including parameter uncertainty. We observe that utilities are the lowest when interest rates are negative. This causes the discounted future claims (liability) to increase and thus decrease the coverage ratio. The yield curve is very persistent, thus a generation that builds up their pension during a low interest rate period ends up with a low utility. The question remains whether the asymptotic distribution of the parameter estimates is realistic. Parameter uncertainty causes negative rates to be fairly present in our scenario set. Negative rates are, historically, not as common as positive rates and are usually used as a monetary policy to stimulate economic growth. It is probable that extreme negative interest are less likely to happen, especially at longer maturities. However, negative rates at longer maturities are present in our scenario set. This is likely due to the data that was used to calibrate the KNW-model. For a majority of our data set short-term interest are close to zero and even negative. This brings us to a present problem that is being faced by the Dutch Central Bank and Committee Parameters as well (Gelderman et al., 2022): the choice of the historical data to calibrate the model. Longer historical data gives us more information about the possible range of the economy. However, using only more recent data gives us a more accurate relationship of the current dynamics of the economy. It is up to Committee Parameters to make a choice in what data to use, but incorporating parameter uncertainty, nonetheless, allows us to model a wider range of the economy.

Further, the parameters are drawn from a normal distribution with an estimated (asymptotic) covariance matrix. The estimation of the covariance matrix requires us to use numerical computations for the second-order derivative. This might create numerical inconsistencies as the numerical approximation of the derivatives might not be so accurate for large functions. One possible method is to solve the derivatives analytically. This can be an interesting approach for further research and will result in a more accurate covariance matrix.

Another approach is to not opt for the asymptotic distribution of the parameters, but take a Bayesian approach into account. Bayesian methods give a posterior distribution of the parameters directly. The literature on Bayesian methods for stochastic differential equations is sparse. Ge (2002) provide some work on Bayesian calibration for stochastic volatility models. Bunnin et al. (2002) present a Bayesian method for option pricing. Särkkä et al. (2006) provides a more

broad overview of recursive Bayesian inference on stochastic differential equations. A Bayesian framework can be useful for the KNW-model as it is currently already working with parameter restrictions. Prior beliefs can be incorporated in the model to incorporate expert views, by e.g. policy makers.

7 Conclusion

In this thesis we look at scenario based policy research under parameter uncertainty. Chen et al. (2019) and Darmoutomo et al. (2020) conduct research to whether age dependent risk allocation leads to welfare gains. Their research measures this by the certainty equivalent of consumption for different risk allocation methods. They show that two out of the three allocation rules led to welfare gains over uniform risk allocation. We question whether the welfare gains are still present when considering parameter uncertainty. This research is two-fold and consists of a model calibration part as well as the scenario based policy research under parameter uncertainty.

First, we calibrate the KNW-model on Dutch economic data, consisting of the MSCI index, HICP index and yields with maturities of 1, 5, 10, 15, 20 and 30 years. There are two different calibration, one without any restrictions, and one with restrictions recommended by Committee Parameters (Dijsselbloem et al., 2019). We find similar results for both models, however the parameters K and Λ show lower absolute values for the restricted calibration. The restricted KNW-model is chosen to generate the economic scenarios. We compare two economic scenarios generated by the restricted KNW-model. For one generation standard errors are not taken into consideration, for the other one we generate economic scenarios based on the asymptotic distribution of the parameters.

Second, the economic scenarios are used to evaluate the welfare gains of age-dependent risk sharing for pension funds. We find results in line with Chen et al. (2019), the 3-2-1 distribution rule leads to a welfare loss of 1.79% and the other two methods uniform adjustment in achievable pension and optimisation over the life cycle lead to welfare gains of around 2.59% and 3.09% respectively. However, we find that when we incorporate parameter uncertainty the welfare gains vanish. The 3-2-1 distribution rule shows a welfare loss and the welfare gains for the other two levels are no longer statistically different from zero at the 10% significance level. The scenario set with parameter uncertainty results into scenarios with fatter-tails and a higher percentage of negative yields.

This research shows that parameter uncertainty plays an important role in scenario based policy research. If we do not consider parameter uncertainty, the scenario set does not represent extreme scenarios well enough. Parameter uncertainty should be considered when generating

economic scenarios. We show this with an example on a policy research by Chen et al. (2019) and Darmoutomo et al. (2020), but it serves purpose outside the scope of this policy research. We suggest further research can look into how this affects other research that is based on economic scenarios. Taking parameter uncertainty into account could lead to more realistic uncertainty for risk models as well as derivative pricing.

References

- Arrow, K. J. (1965), *Aspects of the Theory of Risk-bearing*, Yrjö Jahnessonin Säätiö.
- Benzoni, L., Collin-Dufresne, P. and Goldstein, R. S. (2007), ‘Portfolio choice over the life-cycle when the stock and labor markets are cointegrated’, *The Journal of Finance* **62**(5), 2123–2167.
- Bodie, Z., Merton, R. C. and Samuelson, W. F. (1992), ‘Labor supply flexibility and portfolio choice in a life cycle model’, *Journal of economic dynamics and control* **16**(3-4), 427–449.
- Boelaars, I., Cox, R., Lever, M. and Mehlkopf, R. (2015), ‘The allocation of financial risks during the life cycle in individual and collective dc pension contracts’.
- Boelaars, I. and Mehlkopf, R. (2018), ‘Optimal risk-sharing in pension funds when stock and labor markets are co-integrated’.
- Bovenberg, A. L. and Meijdam, L. (2001), The Dutch Pension System, in ‘Pension Reform in Six Countries’, Springer, pp. 39–67.
- Bovenberg, L., Koijen, R., Nijman, T. and Teulings, C. (2007), ‘Saving and Investing over the Life Cycle and the Role of Collective Pension Funds’, *De Economist* **155**(4), 347–415.
- Bunnin, F. O., Guo, Y. and Ren, Y. (2002), ‘Option pricing under model and parameter uncertainty using predictive densities’, *Statistics and Computing* **12**(1), 37–44.
- Caines, P. E. (2018), *Linear stochastic systems*, SIAM.
- Chen, D., Doll, M. and van Ool, A. (2019), De Toegevoegde Waarde van Maatwerk in Risico-toedeling, Technical report, De Nederlandsche Bank.
- Dai, Q. and Singleton, K. J. (2000), ‘Specification analysis of affine term structure models’, *The journal of finance* **55**(5), 1943–1978.
- Darmoutomo, M., Hoogteijling, T., Honig, W. and Jong, V. (2020), ‘Age Dependent Risk Allocation in the Dutch Pension System’.
- Dijsselbloem, J., De Waegenaere, A., van Ewijk, C., van der Horst, A., Knoef, M. and Steenbeek, O. (2019), ‘Advies commissie parameters’.
- Dillingh, R., Lanser, D. and Lever, M. (2018), Effecten van Afschaffing van de Doorsneesystematiek en de Gelijktijdige Overgang naar een Nieuw Pensioencontract, Technical report, Centraal Planbureau.

- Draper, N. (2012), ‘A Financial Market Model for the US and the Netherlands’.
- Draper, N. (2014), ‘A financial market model for the netherlands’.
- Ge, X. (2002), *Bayesian calibration of stochastic volatility models*, The University of North Carolina at Chapel Hill.
- Gelderman, M., Bonenkamp, J., Diris, B., van Hoogdalem, S., Pelsser, A., Vellekoop, M. and Werker, B. (2022), ‘Rapport Technische werkgroep economische scenario’s’.
- Gomes, F. J., Kotlikoff, L. J. and Viceira, L. M. (2008), ‘Optimal life-cycle investing with flexible labor supply: A welfare analysis of life-cycle funds’, *American Economic Review* **98**(2), 297–303.
- Koijen, R. S., Nijman, T. E. and Werker, B. J. (2010), ‘When can life cycle investors benefit from time-varying bond risk premia?’, *The review of financial studies* **23**(2), 741–780.
- Langejan, T., Gelauff, G., Nijman, T., Sleijpen, O. and Steenbeek, O. (2014), ‘Advies commissie parameters’, *Publicatie Rijksoverheid*.
- Lever, M. and Michelsen, T. (2016), *Welvaartswinst van Risicodeling in een Collectief Pensioenplan*, Technical report, Centraal Planbureau.
- Mehlkopf, R., Bonenkamp, J., van Ewijk, C., ter Rele, H. and Westerhout, E. (2013), ‘Impliciete en expliciete leeftijdsdifferentiatie in pensioencontracten’, *Netspar Design Paper* (13).
- Merton, R. C. (1969), ‘Lifetime portfolio selection under uncertainty: The continuous-time case’, *The review of Economics and Statistics* pp. 247–257.
- Merton, R. C. (1975), Optimum Consumption and Portfolio Rules in a Continuous-time Model, in ‘Stochastic Optimization Models in Finance’, Elsevier, pp. 621–661.
- Modigliani, F. (1966), ‘The Life Cycle Hypothesis of Saving, the Demand for Wealth and the Supply of Capital’, *Social research* pp. 160–217.
- Muns, S. (2015), ‘A financial market model for the Netherlands: A methodological refinement’.
- Muns, S. and Werker, B. (2019), ‘Baten van Slimme Toedeling Rendementen Hoger dan van Intergenerationele Risicodeling’, *Economisch Statistische Berichten: Algemeen Weekblad voor Handel, Nijverheid, Financiën en Verkeer* **104**(4777), 427–429.
- Pelsser, A. (2019), ‘Kalman Filter Estimation of the KNW Model’, *Available at SSRN 3885556*

- Pratt, J. W. (1964), 'Risk Aversion in the Large and in the Small', *Econometrica* **32**(1), 132–136.
- Samuelson, P. A. (1975), 'Lifetime portfolio selection by dynamic stochastic programming', *Stochastic optimization models in finance* pp. 517–524.
- Särkkä, S. et al. (2006), *Recursive Bayesian inference on stochastic differential equations*, Helsinki University of Technology.
- Teulings, C. N. and De Vries, C. G. (2006), 'Generational Accounting, Solidarity and Pension Losses', *De Economist* **154**(1), 63–83.
- Viceira, L. M. (2001), 'Optimal portfolio choice for long-horizon investors with nontradable labor income', *The Journal of Finance* **56**(2), 433–470.

Appendices

A Code structure

All code was written in MATLAB and is publicly available on GitHub at https://github.com/MichaelDarmoutomo/thesis_matlab.

```
/thesis_matlab
├── data
│   ├── economy_cov.mat
│   ├── se.mat
│   ├── se_restricted.mat
│   ├── x_opt.mat
│   └── x_opt_restricted.mat
├── kalman_filter
│   ├── GetParameters.m
│   ├── KalmanFilter.m
│   ├── KalmanParameters.m
│   ├── KalmanSmoother.m
│   └── LogLikelihood.m
├── pension_fund
│   ├── GenerateEconomy.m
│   ├── GenerateEconomySE.m
│   ├── PensionFund.m
│   └── PensionFundSE.m
├── toolboxes
├── main_kalman.m
├── main_pension_fund.m
├── pension_fund_cec.m
└── pension_fund_std.m
```

We will briefly describe the folders and main scripts.

data Folder containing all the data for this thesis.

kalman_filter Folder with relevant functions for estimating the Kalman filter.

pension_fund Folder with relevant functions to simulate the economies as well as the pension fund.

`main_kalman.m` Pipeline script to estimate the KNW-model.

`main_pension_fund.m` Pipeline script to run the pension fund modeling.

`pension_fund_cec.m` Script to compute the CEC and standard errors over the optimal parameters.

`pension_fund_std.m` Script to compute the CEC and standard errors over the optimal parameters with simulation with standard errors.

B Scenario sets

This section shows histograms of inflation, short rates and stock returns for two different scenario sets.

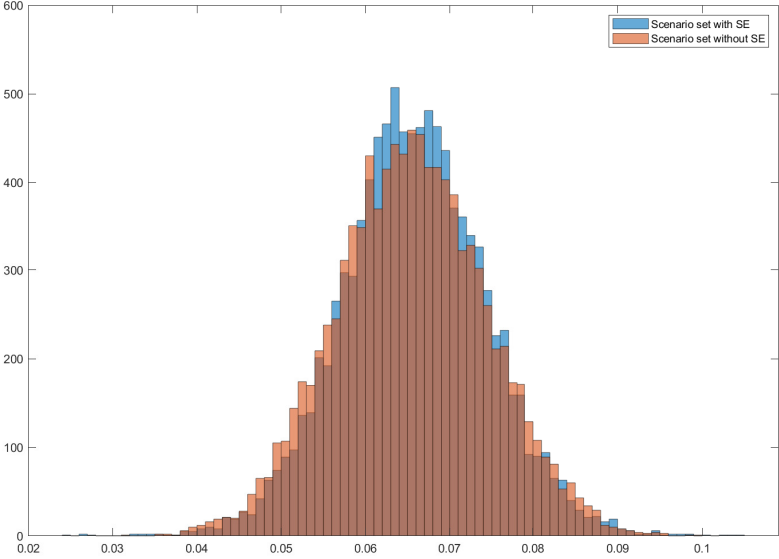


Figure 4: Stock index returns. This figure shows a histogram of the average stock index return for each simulation. The blue bars show the returns for scenario set where standard errors were incorporated, and the orange bars show the returns for the simulation based on the point-estimates.

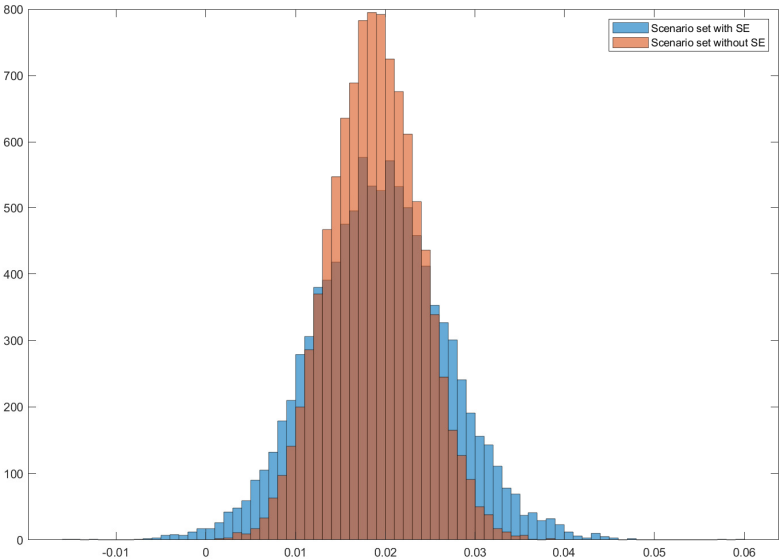


Figure 5: Short rate returns. This figure shows a histogram of the average short rate return for each simulation. The blue bars show the returns for scenario set where standard errors were incorporated, and the orange bars show the returns for the simulation based on the point-estimates.

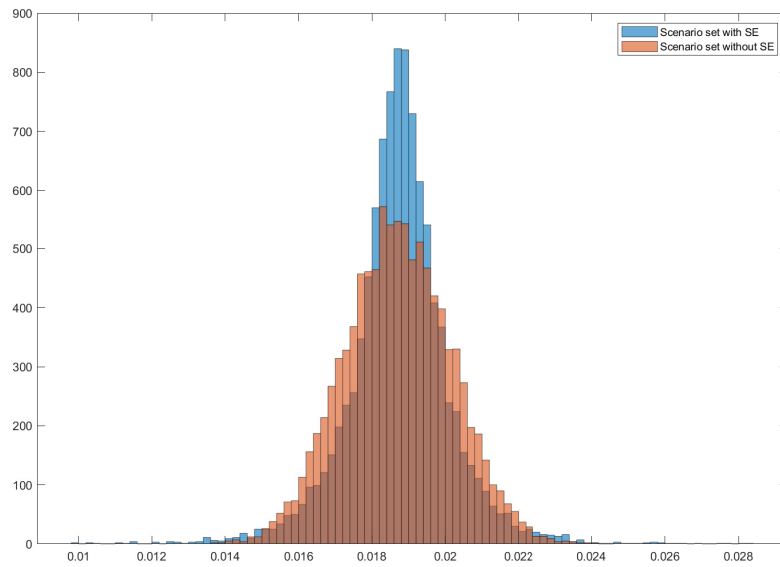


Figure 6: Change in inflation. This figure shows a histogram of the changes in inflation for each simulation. The blue bars show the changes for scenario set where standard errors were incorporated, and the orange bars show the changes for the simulation based on the point-estimates.